Port-Hamiltonian Based Control of the Sun-Earth 3D Circular Restricted Three-Body Problem: Stabilization of the L_1 Lagrange Point

Haotian Yan

Community School of Naples, Virginia, USA
Email: yhtbaoyuan@163.com

Abstract

In this paper, we use Port-Hamiltonian framework to stabilize the Lagrange points in the Sun-Earth three-dimensional Circular Restricted Three-Body Problem (CRTBP). Through rewriting the CRTBP into Port-Hamiltonian framework, we are allowed to design the feedback controller through energy-shaping and dissipation injection. The closed-loop Hamiltonian is a candidate of the Lyapunov function to establish nonlinear stability of the designed equilibrium, which enlarges the application region of feedback controller compared with that based on linearized dynamics. Results show that the Port-Hamiltonian approach allows us to successfully stabilize the Lagrange points, where the Linear Quadratic Regulator (LQR) may fail. The feedback system based on Port-Hamiltonian approach is also robust against white noise in the inputs.

Keywords

1. Introduction

The Circular Restricted Three Body Problem (CRTBP) [1] has been widely studied by physicists, astronomers, and astrodynamics. This problem is focused on overcoming the difficulties in finding a suitable orbit for satellites. In the system of the CRTBP, there exist five equilibrium positions, which are known as Lagrange points. These Lagrange points are of scientific and engineering interest; e.g., artificial spacecrafts have been placed at the L_1 and L_2 Lagrange points with respect to the Sun and the Earth [2] [3] [4] [5] and Lagrange points with respect

to the Earth and the Moon [6] [7].

However, that is also of the most demanding challenge; *i.e.*, among the five Lagrange points, three of them are unstable [1] [8]. Fortunately, around these unstable points (L_1, L_2, L_3), there exist stable halo orbits, which allow artificial satellite to reside. In order to design an orbit around Lagrange points, the most broadly used methods are based on linearization around a halo orbit or Lagrange point [9] [10] [11] [12] [13].

However, stabilization of a linear system is only able to guarantee the stability of the system against an infinitely small perturbation, but is unable to guarantee the stability against a finite disturbance. Disturbances for the Earth-Moon Lagrange points mission under CRTBP model include the eccentricity of the Earth-Moon orbit, the gravity from the other bodies [14] and the solar radiation pressure. For the Sun-Earth Lagrange points mission, the perturbation from the Moon is critical. Lyapunov [15], in the year of 1895, proposed the Lyapunov method to establish the stability of nonlinear system. The difficulties of Lyapunov's method is finding a Lyapunov function to establish the stability. For Hamiltonian system, the conserved quantity Hamiltonian is a candidate of Lyapunov function to establish the stability of the system. The Jacobian integral [16], which is the conserved quantity for the CRTBP in a rotating coordinate, allows us to formulate the CRTBP as the Hamiltonian system.

Port-Hamiltonian system [17] [18] generalizes the Hamiltonian system and allows us to take input and dissipation into consideration, which are described as "port". This framework has the potential to model, analyze and especially, control complex physical systems and their interconnections [17]. The Port-Hamiltonian framework also provides a physics-based control strategy [19]-[24], which focuses on shaping the closed-loop Hamiltonian as the candidate of Lyapunov function.

In this research, we use the Port-Hamiltonian system to reformulate the Sun-Earth three-dimensional CRTBP, which retains the original nonlinear dynamics in contrast to the linear approximation. Then, we designed the feedback control law to stabilize the unstable Lagrange points by taking input and dissipation as two other actors into consideration. The closed-loop Hamiltonian serves as the candidate of Lyapunov's function, which helps to establish the nonlinear stability of the open-loop unstable Lagrange points. This research provides further possibility in Lagrange point launching mission.

2. The Circular Restricted Three Body Problem

2.1. Governing Equations

In Circular Restricted Three Body Problem (CRTBP), it requires the largest two objects of the three have a significantly larger mass compared to the third one; *i.e.*, $M_1 \gg M_3$ and $M_2 \gg M_3$. The largest two objects are in circular orbits centered at their center of mass. We consider the third object, M_3, moving in three-dimensional (3D) space; *i.e.*, 3D-CRTBP. In order to solve this problem,

we need to use mathematical method to approximate this situation. We set the center of mass of the system as the origin and we set the position of M_1 at $(-\mu, 0)$, position of M_2 at $(1-\mu, 0)$, where we define $\mu = M_2/M$ and $M = M_1 + M_2$. Then, the dynamics of the third body can be described as [1]:

$$\frac{d^2x}{dt^2} - 2\frac{dy}{dt} = x - (1-\mu)\frac{x+\mu}{r_1^3} - \mu\frac{x-1+\mu}{r_2^3} \tag{1}$$

$$\frac{d^2y}{dt^2} + 2\frac{dx}{dt} = y - (1-\mu)\frac{y}{r_1^3} - \mu\frac{y}{r_2^3} \tag{2}$$

$$\frac{d^2z}{dt^2} = -\left(\frac{1-\mu}{r_1^3} - \frac{\mu}{r_2^3}\right)z \tag{3}$$

where

$$r_1 = \sqrt{(x+\mu)^2 + y^2 + z^2} \tag{4}$$

$$r_2 = \sqrt{(x-1+\mu)^2 + y^2 + z^2} \tag{5}$$

We set $\mu = 3.003490055444426 \times 10^{-6}$, which is the mass ratio in the Sun-Earth CRTBP system (see Table 1).

2.2. The Lagrange Points and the Jacobian Integral

Lagrange points are points in systems on which the third object could reach equilibrium state. According to [1], there exists five Lagrange points in the CRTBP. Three of the five points, L_1, L_2, and L_3 can be computed using algebraic equations:

$$x - (1-\mu)\frac{x+\mu}{r_1^3} - \mu\frac{x-1+\mu}{r_2^3} = 0 \tag{6}$$

$$y = 0 \tag{7}$$

In CRTBP, Jacobian integral is the only conserved variable, which is widely used to derive solutions in special cases, and is expressed as what follows in the (x, y)-coordinate system:

$$C = (x^2 + y^2) + 2\left(\frac{1-\mu}{r_1} + \frac{\mu}{r_2}\right) - (x^2 + y^2 + z^2) \tag{8}$$

Conservation of energy (kinetic energy and potential energy) is shown by Jacobian integral in CRTBP under synodic coordinates description, in which the dissipation caused by the air drag is not included in the model.

Table 1. Lagrange points for the Sun-Earth CRTBP with $\mu = 3.003490055444426 \times 10^{-6}$.

	L_1	L_2	L_3	L_4	L_5
x	0.990026583427689	1.010034125978081	1.000001251454178	0.499996996509945	0.499996996209945
y	0	0	0	0.866025403784439	0.866025403784439

3. Port-Hamiltonian System

3.1. Reformulation of CRTBP

If we use the Hamiltonian proportional to the Jacobian integral:

$$H = -\frac{C}{2} = \frac{1}{2}\left(\dot{x}^2 + \dot{y}^2 + \dot{z}^2\right) - \frac{1}{2}\left[2\left(\frac{1-\mu}{r_1} + \frac{\mu}{r_2}\right) + \left(x^2 + y^2\right)\right] \tag{9}$$

We can reformulate the CRTBP into Port-Hamiltonian system description:

$$\frac{\mathrm{d}}{\mathrm{d}t}x = [J - R]\nabla_x H(x) + Bu \tag{10}$$

where $x = \begin{bmatrix} x\ y\ z\ \dot{x}\ \dot{y}\ \dot{z} \end{bmatrix}^{\mathrm{T}}$ are state variables and $u = \begin{bmatrix} u_x\ u_y\ u_z \end{bmatrix}^{\mathrm{T}}$ are inputs representing thrust force on x, y and z directions. In order to map inputs to state variables, we define $B = \begin{bmatrix} 0 & 0 & 0 & 1 & 0 & 0 \\ 0 & 0 & 0 & 0 & 1 & 0 \\ 0 & 0 & 0 & 0 & 0 & 1 \end{bmatrix}^{\mathrm{T}}$. J is a skew-symmetric matrix, which represents the energy conserving part, while matrix R is a symmetric positive semi-definite matrix, which represents the energy dissipation:

$$J = \begin{bmatrix} 0 & 0 & 0 & 1 & 0 & 0 \\ 0 & 0 & 0 & 0 & 1 & 0 \\ 0 & 0 & 0 & 0 & 0 & 1 \\ -1 & 0 & 0 & 0 & 2 & 0 \\ 0 & -1 & 0 & -2 & 0 & 0 \\ 0 & 0 & -1 & 0 & 0 & 0 \end{bmatrix}^{\mathrm{T}}, \quad R = 0_{6\times 6} \tag{11}$$

Since CRTBP does not consider energy dissipation such as air drag, R is a zero matrix. This causes the conservation of energy (Hamiltonian or Jacobian integral used here), which is the fact reflected in the following equation:

$$\begin{aligned}
\frac{\mathrm{d}H(x)}{\mathrm{d}t} &= \nabla_x H(x) \cdot \frac{\mathrm{d}x}{\mathrm{d}t} = \nabla_x H(x) \cdot [J - R]\nabla_x H(x) \\
&= \nabla_x H(x) \cdot [-R]\nabla_x H(x) = 0
\end{aligned} \tag{12}$$

3.2. Energy Shaping

Instead of controlling the Hamiltonian, we are focused on reshaping the Hamiltonian in CRTBP, where the equilibrium points $x^* = \begin{bmatrix} x^*\ y^*\ z^*\ 0\ 0\ 0 \end{bmatrix}^{\mathrm{T}}$ are stable. Thus, we designed a closed-loop Hamiltonian $H_d(x)$:

$$H_d(x) = \frac{1}{2}\left[\dot{x}^2 + \dot{y}^2 + \dot{z}^2 + \left(x - x^*\right)^2 + \left(y - y^*\right)^2 + \left(z - z^*\right)^2\right] \tag{13}$$

with the minimal position:

$$x^* = \arg\min\{H_d(x)\} \tag{14}$$

assuming that the closed loop system is also a Port-Hamilton system

$$\frac{\mathrm{d}x}{\mathrm{d}t} = [J - R]\nabla_x H_d \tag{15}$$

Then, we design the feedback control law as $\boldsymbol{B}$ is full column rank but not full row rank:

$$\boldsymbol{u}_{ES}(\boldsymbol{x}) = (\boldsymbol{B}^{\mathrm{T}}\boldsymbol{B})^{-1}\boldsymbol{B}^{\mathrm{T}}[\boldsymbol{J}-\boldsymbol{R}]\nabla_x H_a(\boldsymbol{x}) \tag{16}$$

$$H_a(\boldsymbol{x}) = H_d(\boldsymbol{x}) - H(\boldsymbol{x}) \tag{17}$$

where the difference between close-loop system and open-loop system is shown by

$$\boldsymbol{B}^{\perp}[\boldsymbol{J}-\boldsymbol{R}]\nabla_x H_a(\boldsymbol{x}) = \boldsymbol{0} \tag{18}$$

Under this control law, it can be shown that the closed-loop Hamiltonian is a Lyapunov function satisfying:

$$H_d(\boldsymbol{x}) = 0,\, \boldsymbol{x} = \boldsymbol{x}^* \tag{19}$$

$$H_d(\boldsymbol{x}) > 0,\, \forall \boldsymbol{x} \neq \boldsymbol{x}^* \tag{20}$$

$$\frac{\mathrm{d}H_d(\boldsymbol{x})}{\mathrm{d}t} = \nabla_x H_d(\boldsymbol{x})\cdot[-\boldsymbol{R}]\nabla_x H_d(\boldsymbol{x}) = 0,\, \forall \boldsymbol{x} \neq \boldsymbol{x}^* \tag{21}$$

According to Lyapunov stability theorem, the equilibrium $\boldsymbol{x}$ of the closed-loop system is stable.

3.3. Dissipation Injection

Previous energy shaping process utilizes a state feedback control law to shape the closed-loop Hamiltonian (energy) with a stable equilibrium at $\boldsymbol{x}^*$. However, the closed-loop Hamiltonian also remains a constant; *i.e.*, $\frac{\mathrm{d}H_d(\boldsymbol{x})}{\mathrm{d}t} = \nabla_x H_d(\boldsymbol{x})\cdot[-\boldsymbol{R}]\nabla_x H_d(\boldsymbol{x}) = 0$. We may also design the equilibrium point as asymptotically stable. This can be achieved through dissipation injection, which modifies the $\boldsymbol{R}$ matrix in the closed-loop system. Aside from the energy shaping control law, we also implement a state feedback control representing dissipation injection:

$$\boldsymbol{u}_{DI}(\boldsymbol{x}) = -\boldsymbol{K}_d \boldsymbol{B}^{\mathrm{T}}\nabla_x H_d(\boldsymbol{x}) \tag{22}$$

where $\boldsymbol{K}_d$ is positive definite. With $\boldsymbol{u}(\boldsymbol{x}) = \boldsymbol{u}_{ES}(\boldsymbol{x}) + \boldsymbol{u}_{DI}(\boldsymbol{x})$, we have the closed-loop system as:

$$\frac{\mathrm{d}x}{\mathrm{d}t} = [\boldsymbol{J} - \boldsymbol{R}_d(\boldsymbol{x})]\nabla_x H_d \tag{23}$$

with a closed-loop dissipation matrix: $\boldsymbol{R}_d(\boldsymbol{x}) = \boldsymbol{R}(\boldsymbol{x}) + \boldsymbol{B}(\boldsymbol{x})\boldsymbol{K}_d\boldsymbol{B}^{\mathrm{T}}$.

Thus, the closed-loop Hamiltonian evolves like:

$$\frac{\mathrm{d}H_d(\boldsymbol{x})}{\mathrm{d}t} = \nabla_x H_d(\boldsymbol{x})\cdot[-\boldsymbol{R}_d]\nabla_x H_d(\boldsymbol{x}) \leq 0,\, \forall \boldsymbol{x} \neq \boldsymbol{x}^* \tag{24}$$

The closed-loop Hamiltonian $H_d(\boldsymbol{x})$ also satisfies $H_d(\boldsymbol{x}) = 0$, $\boldsymbol{x} = \boldsymbol{x}^*$ and $H_d(\boldsymbol{x}) > 0$, $\forall \boldsymbol{x} = \boldsymbol{x}^*$.

As the union of complete trajectories contained entirely in the set has no trajectory except the trivial one $x(t) = \mathbf{0}$ for $t \geq x^*$, we obtain the asymptotic stability of the closed-loop system according to LaSalle's invariance principle [25]. The above framework of energy shaping and dissipation injection are summarized as Figure 1.

4. Results and Discussion

Figures 2-4 shows the orbit of the third body without background noise on x-y, x-z, and y-z plane, respectively. The blue dashed lines in these figures indicated the controlled orbits using (a) Linear Quadratic Regulator (LQR) controller compared with (b) Port-Hamiltonian controller. The results show that the Port-Hamiltonian controller allows us to drive the third body to the target equilibrium position, while the LQR controller fail. The LQR controller is designed [11] [26] [27] according to the CRTBP linearized around the L_1 Lagrange point: $\frac{dx}{dt} = Ax + Bu$ where A is the Jacobian of $(J - R)\nabla H(x)$ evaluated at the equilibrium point x^*; i.e. the first Lagrange point L_1 in this case. Using the Linear Quadratic Regulator (LQR) controller, we obtain the control law as $u_{LQR} = -K(x - x^*)$, where K minimizes the cost function $J_{LQR} = \int_0^\infty x^T Q x + u^T R u$ with $Q = I_{6\times6}$ and $R = I_{3\times3}$.

Figures 5-7 shows the orbit of the third body with background noise on x-y, x-z, and y-z plane, respectively. This background noise is used to model the disturbance including eccentricity of the orbit, the gravity from the other bodies [14]. Especially, for the Sun-Earth Lagrange points mission, the perturbation from the Moon is critical. The results show that, under the background noise, the Linear Quadratic Regulator is not able to drive the third body to the target position; i.e., L_1 Lagrange point in the Sun-Earth CRTBP. However, the approach based on the Port-Hamiltonian successfully drive the third body to the targeting position.

Figure 8 & Figure 9 show the time history of the controller inputs u_x, u_y and u_z without background noise and with background noise, respectively. Results indicate that the controller input for Port-Hamiltonian controller is asymptoting to zero as the third body is approaching the target location, in consistent with the observation of previous results. These results indicate that when the third body is approaching the target position or the disturbance is small, the required control input is also small.

$$u = u_{ES} + u_{DI}$$

$$\frac{d}{dt}x = [J - R]\nabla_x H + Bu \quad \Rightarrow \quad \frac{d}{dt}x = [J - R_d]\nabla_x H_d$$

$$x^* = \arg\min H_d \qquad \frac{dH_d}{dt} < 0$$
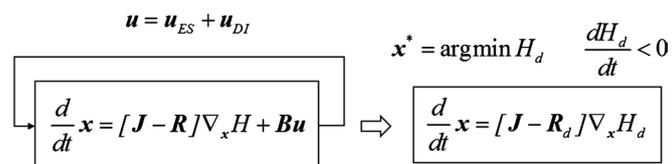
Figure 1. The flow chart of energy shaping and dissipation injection. Where $H(x)$ is a Hamiltonian, $H_d(x)$ is a closed-loop Hamiltonian, matrix R is a symmetric positive semi-definite matrix which represents the energy dissipation and $R_d = R + B(x)K_d B^T$.
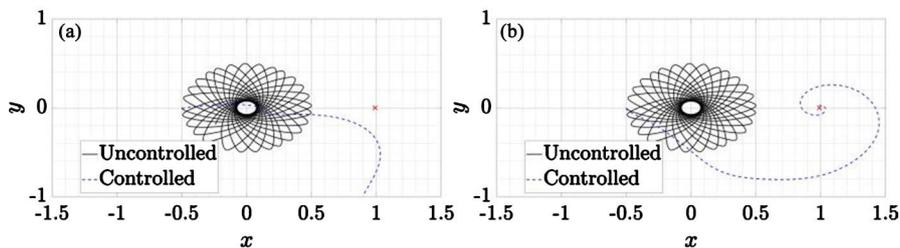
Figure 2. The orbit of the third body on *x-y* plane without background noise. The black solid line represents the uncontrolled orbit, and the red cross represents L_1 Lagrange point. The blue dashed line represents the controlled orbit with (a) LQR controller and (b) port-Hamiltonian controller.
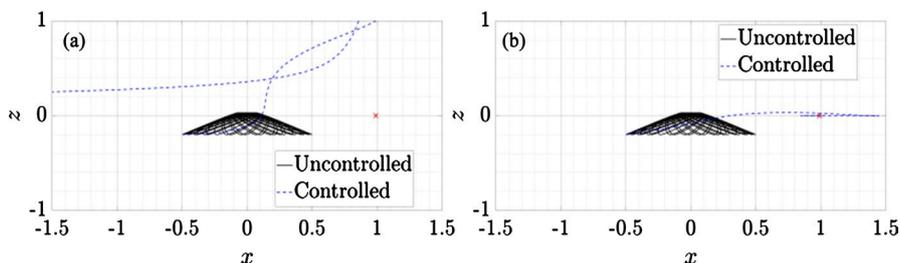
Figure 3. The orbit of the third body on *x-z* plane without background noise. The black solid line represents the uncontrolled orbit, and the red cross represents L_1 Lagrange point. The blue dashed line represents the controlled orbit with (a) LQR controller and (b) port-Hamiltonian controller.
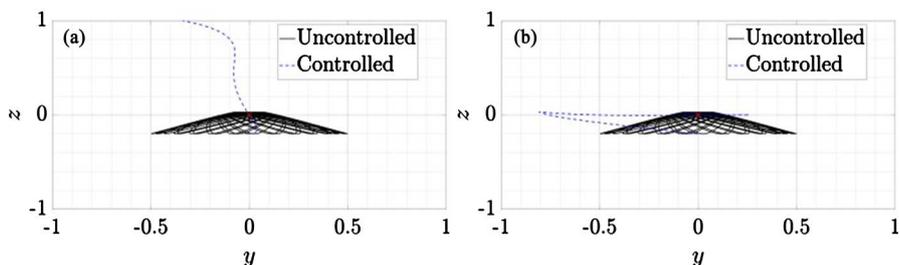
Figure 4. The orbit of the third body on *y-z* plane without background noise. The black solid line represents the uncontrolled orbit, and the red cross represents L_1 Lagrange point. The blue dashed line represents the controlled orbit with (a) LQR controller and (b) port-Hamiltonina controller.
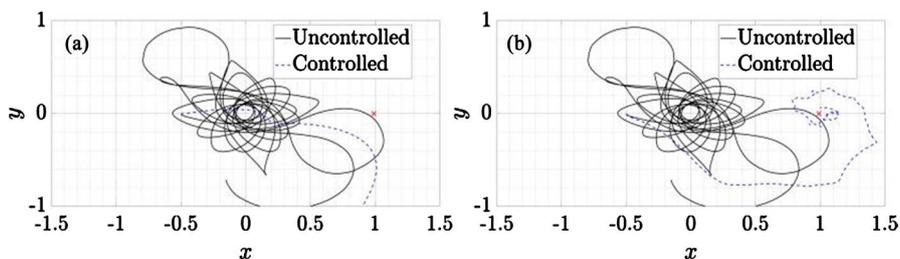
Figure 5. The orbit of the third body on *x-y* plane with background noise, and the red cross represents L_1 Lagrange point. The black solid line represents the uncontrolled orbit; the blue dashed line represents the controlled orbit with (a) LQR controller compared with (b) port-Hamiltonian controller.
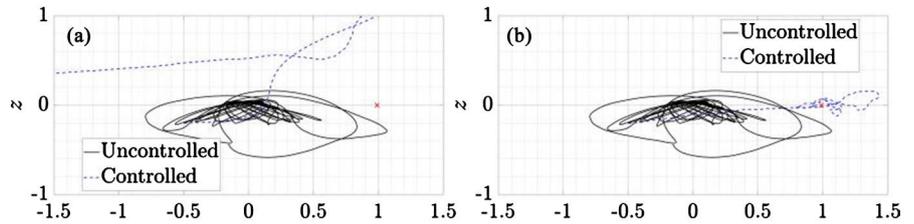
Figure 6. The orbit of the third body on *x-z* plane with background noise. The black solid line represents the uncontrolled orbit, and the red cross represents L_1 Lagrange point. The blue dashed line represents the controlled orbit with (a) LQR controller and (b) port-Hamiltonian controller.
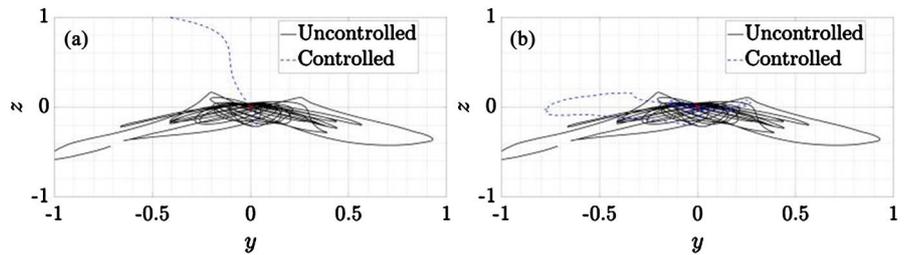
Figure 7. The orbit of the third body on *y-z* plane with background noise. The black solid line represents the uncontrolled orbit, and the red cross represents L_1 Lagrange point. The blue dashed line represents the controlled orbit with (a) LQR controller and (b) port-Hamiltonian controller.
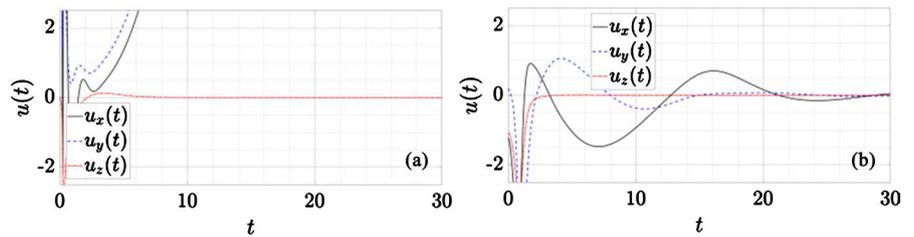
Figure 8. The control input according to the (a) LQR controller and (b) port-Hamiltonian controller without background noise.
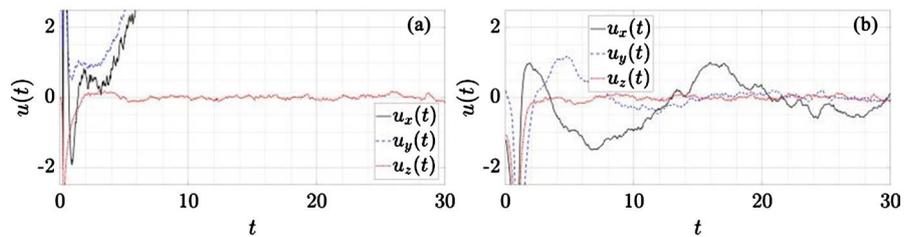
Figure 9. The control input according to the (a) LQR controller and (b) port-Hamiltonian controller with background noise.

5. Conclusion

In this paper, we use Port-Hamiltonian framework to stabilize the Lagrange points in the Circular Restricted Three-Body Problem (CRTBP). Through exploring the energy (Jacobi integral) conserving property in CRTBP, this problem is rewritten

into Port-Hamiltonian framework, where we use the Jacobi integral as the Hamiltonian. Then, we design the feedback controller through energy-shaping and dissipation injection to stabilize the L_1 Lagrange point of the Sun-Earth CRTBP. The closed-loop Hamiltonian is designed as the candidate of the Lyapunov function to establish nonlinear stability of the designed equilibrium, which enlarges the application region of feedback controller compared with that based on linearized dynamics. Results show that the Port-Hamiltonian approach allows us to successfully stabilize the Lagrange points, where the Linear Quadratic Regulator (LQR) may fail. Adding the white noise into the inputs, the designed feedback controller based on Port-Hamiltonian approach also allows us to stabilize the Lagrange points, which demonstrates the robustness against the background noise of the designed feedback control.

Acknowledgements

Conflicts of Interest

The author declares no conflicts of interest regarding the publication of this paper.

References

[1] Musielak, Z.E. and Quarles, B. (2014) The Three-Body Problem. *Reports on Progress in Physics*, **77**, Article ID: 065901.
https://doi.org/10.1088/0034-4885/77/6/065901

[2] Pilbratt, G.L., Riedinger, J.R., Passvogel, T., Crone, G., Doyle, D., Gageur, U., Heras, A.M., Jewell, C., Metcalfe, L., Ott, S., *et al.* (2010) Herschel Space Observatory. An ESA Facility for Far-Infrared and Submillimetre Astronomy. A*stronomy & Astrophysics*, **518**, Article No. L1. https://doi.org/10.1051/0004-6361/201014759

[3] Gardner, J.P., Mather, J.C., Clampin, M., Doyon, R., Greenhouse, M.A., Hammel, H.B., Hutchings, J.B., Jakobsen, P., Lilly, S.J., Long, K.S., *et al.* (2006) The James Webb Space Telescope. S*pace Science Reviews*, **123**, 485-606.
https://doi.org/10.1007/s11214-006-8315-7

[4] Farquhar, R. (1998) The Flight of ISEE-3/ICE-Origins, Mission History, and a Legacy. *AIAA/AAS Astrodynamics Specialist Conference and Exhibit*, Boston, 10-12 August 1998, 4464. https://doi.org/10.2514/6.1998-4464

[5] Stone, E.C., Frandsen, A.M., Mewaldt, R.A., Christian, E.R., Margolies, D., Ormes, J.F. and Snow, F. (1998) The Advanced Composition Explorer. *Space Science Reviews*, **86**, 1-22. https://doi.org/10.1023/A:1005082526237

[6] Sweetser, T.H., Broschart, S.B., Angelopoulos, V., Whiffen, G.J., Folta, D.C., Chung, M.K., Hatch, S.J. and Woodard, M.A. (2012) ARTEMIS Mission Design. In: Russell, C. and Angelopoulos, V., Eds., *The ARTEMIS Mission*, Springer, New York, 61-91.
https://doi.org/10.1007/978-1-4614-9554-3_4

[7] Shirobokov, M., Trofimov, S. and Ovchinnikov, M. (2017) Survey of Station-Keeping Techniques for Libration Point Orbits. *Journal of Guidance, Control, and Dynamics*,

40, 1085-1105. https://doi.org/10.2514/1.G001850

[8] Meyer, K.R. and Schmidt, D.S. (1986) The Stability of the Lagrange Triangular Point and a Theorem of Arnold. *Journal of Differential Equations*, **62**, 222-236. https://doi.org/10.1016/0022-0396(86)90098-7

[9] Gómez, G., Jorba, A., Masdemont, J. and Simó, C. (1993) Study of the Transfer from the Earth to a Halo Orbit around the Equilibrium point L_1. *Celestial Mechanics and Dynamical Astronomy*, **56**, 541-562. https://doi.org/10.1007/BF00696185

[10] Richardson, D.L. (1980) Halo Orbit Formulation for the ISEE-3 Mission. *Journal of Guidance, Control, and Dynamics*, **3**, 543-548. https://doi.org/10.2514/3.56033

[11] Cielaszyk, D. and Wie, B. (1996) New Approach to Halo Orbit Determination and Control. *Journal of Guidance, Control, and Dynamics*, **19**, 266-273. https://doi.org/10.2514/3.21614

[12] Ardaens, J.S. and D'Amico, S. (2008) Control of Formation Flying Spacecraft at a Lagrange Point. No. 00-08.

[13] Xu, M. and Xu, S.J. (2008) Trajectory and Correction Maneuver during the Transfer from Earth to Halo Orbit. *Chinese Journal of Aeronautics*, **21**, 200-206. https://doi.org/10.1016/S1000-9361(08)60026-6

[14] Yamato, H. and Spencer, D. (2004) Transit-Orbit Search for Planar Restricted Three-Body Problems with Perturbations. *Journal of Guidance, Control, and Dynamics*, **27**, 1035-1045. https://doi.org/10.2514/1.4524

[15] Lyapunov, A.M. (1992) The General Problem of the Stability of Motion. *International Journal of Control*, **55**, 531-534. https://doi.org/10.1080/00207179208934253

[16] Jacobi, C.G.J. (1836) Sur le mouvement d'un point et sur un cas particulier du probleme destrois corps. *Comptes Rendus Chimie*, **3**, 59-61.

[17] Van Der Schaft, A.J. and Schumacher, J.M. (2000) An Introduction to Hybrid Dynamical Systems. Springer, London, 251. https://doi.org/10.1007/BFb0109998

[18] Van Der Schaft, A.J., Jeltsema, D. *et al.* (2014) Port-Hamiltonian Systems Theory: An Introductory Overview. *Foundations and Trends in Systems and Control*, **1**, 173-378. https://doi.org/10.1561/2600000002

[19] Ortega, R., Van Der Schaft, A.J., Mareels, I. and Maschke, B. (2001) Putting Energy Back in Control. *IEEE Control Systems Magazine*, **21**, 18-33. https://doi.org/10.1109/37.915398

[20] Ortega, R., Van Der Schaft, A.J., Maschke, B. and Escobar, G. (2002) Interconnection and Damping Assignment Passivity-Based Control of Port-Controlled Hamiltonian Systems. *Automatica*, **38**, 585-596. https://doi.org/10.1016/S0005-1098(01)00278-3

[21] Ortega, R., Van Der Schaft, A.J., Castanos, F. and Astolfi, A. (2008) Control by Interconnection and Standard Passivity-Based Control of Port-Hamiltonian Systems. *IEEE Transactions on Automatic Control*, **53**, 2527-2542. https://doi.org/10.1109/TAC.2008.2006930

[22] Liu, C. (2019) Teaching Control Theory in Physics: The Port-Hamiltonian Framework. *College Physics*, **38**, 1-7.

[23] Liu, C. and Dong, L. (2019) Physics-Based Control Education: Energy, Dissipation, and Structure Assignments. *European Journal of Physics*, **40**, Article ID: 035006. https://doi.org/10.1088/1361-6404/ab03e8

[24] Liu, C. and Dong, L. (2019) Stabilization of Lagrange Points in Circular Restricted Three-Body Problem: A Port-Hamiltonian Approach. *Physics Letters A*, **383**, 1907-1914. https://doi.org/10.1016/j.physleta.2019.03.033

[25] LaSalle, J. (1960) Some Extensions of Liapunov's Second Method. *IRE Transactions on Circuit Theory*, **7**, 520-527. https://doi.org/10.1109/TCT.1960.1086720

[26] Kwakernaak, H. and Sivan, R. (1972) Linear Optimal Control Systems. Wiley-Interscience, New York.

[27] Zhou, K., Doyle, J.C., Glover, K., *et al.* (1996) Robust and Optimal Control. Prentice Hall, Upper Saddle River.